



All reported non-canonical splice site variants in *GLA* cause aberrant splicing

Eri Okada^{1,2} · Tomoko Horinouchi¹ · Tomohiko Yamamura¹ · Yuya Aoto¹ · Ryota Suzuki^{1,3} · Yuta Ichikawa¹ · Yu Tanaka¹ · Chika Masuda¹ · Hideaki Kitakado¹ · Atsushi Kondo¹ · Nana Sakakibara¹ · Shinya Ishiko¹ · China Nagano¹ · Shingo Ishimori¹ · Joichi Usui² · Kunihiro Yamagata² · Masafumi Matsuo⁴ · Kandai Nozu¹

Received: 26 January 2023 / Accepted: 14 May 2023 / Published online: 31 May 2023
© The Author(s) 2023

Abstract

Background Fabry disease is an X-linked lysosomal storage disorder caused by insufficient α -galactosidase A (GLA) activity resulting from variants in the *GLA* gene, which leads to glycosphingolipid accumulation and life-threatening, multi-organ complications. Approximately 50 variants have been reported that cause splicing abnormalities in *GLA*. Most were found within canonical splice sites, which are highly conserved GT and AG splice acceptor and donor dinucleotides, whereas one-third were located outside canonical splice sites, making it difficult to interpret their pathogenicity. In this study, we aimed to investigate the genetic pathogenicity of variants located in non-canonical splice sites within the *GLA* gene.

Methods 13 variants, including four deep intronic variants, were selected from the Human Gene Variant Database Professional. We performed an *in vitro* splicing assay to identify splicing abnormalities in the variants.

Results All candidate non-canonical splice site variants in *GLA* caused aberrant splicing. Additionally, all but one variant was protein-truncating. The four deep intronic variants generated abnormal transcripts, including a cryptic exon, as well as normal transcripts, with the proportion of each differing in a cell-specific manner.

Conclusions Validation of splicing effects using an *in vitro* splicing assay is useful for confirming pathogenicity and determining associations with clinical phenotypes.

Keywords GLA · Fabry disease · Minigene assay · Aberrant splicing · Deep intronic variant · Inherited kidney disease

Introduction

Fabry disease (OMIM no. 301500) is an X-linked lysosomal storage disorder resulting from insufficient α -galactosidase A (GLA; GenBank accession no. 2717) activity caused by mutations in the *GLA* gene at Xq22. An enzymatic defect

in GLA protein results in the accumulation of globotriaosylceramide and related glycosphingolipids throughout the body [1, 2]. Typically, hemizygous males with little (< 1% of normal) or no GLA activity suffer from characteristic abnormalities in multiple organs, namely neurological (acroparesthesia), cutaneous (angiokeratomas), renal (proteinuria, kidney failure), cardiovascular (cardiomyopathy, arrhythmia), and cerebrovascular (stroke) symptoms. This phenotype is known as the "classic type". In contrast, some patients have a somewhat preserved level of enzyme activity, and only display predominant cardiac or renal symptoms later in life; these phenotypes are sub-classified as the "cardiac type" [3, 4] and "renal type" [5], respectively.

To date, 1086 variants of the *GLA* gene have been registered in the Human Gene Mutation Database (HGMD)

✉ Eri Okada
okada.eri.oy@ms.hosp.tsukuba.ac.jp

¹ Department of Pediatrics, Kobe University Graduate School of Medicine, 7-5-1 Kusunoki-Cho, Chuo-Ku, Kobe, Hyogo 650-0017, Japan
² Department of Nephrology, Faculty of Medicine, University of Tsukuba, Tsukuba, Japan
³ Department of Pediatrics, Hokkaido University Graduate School of Medicine, Sapporo, Japan
⁴ Department of Physical Rehabilitation and Research Center for Locomotion Biology, Kobe Gakuin University, Hyogo, Japan

Professional (released in 2021.2) (<https://portal.biobase-international.com/hgmd/pro/start.php>). Among these, approximately 5% correspond to splicing changes that may cause aberrant splicing. Most intronic variants of the *GLA* gene registered in HGMD are located at canonical splice sites (dinucleotides at each end of the intron, usually GT at the 5'-end and AG at the 3'-end). Generally, these variants within canonical splice sites cause aberrant splicing because they impact highly conserved sequences that determine exon–intron boundaries [6]. Although several reported variants are located outside these canonical splice sites, their pathogenicity is not yet confirmed.

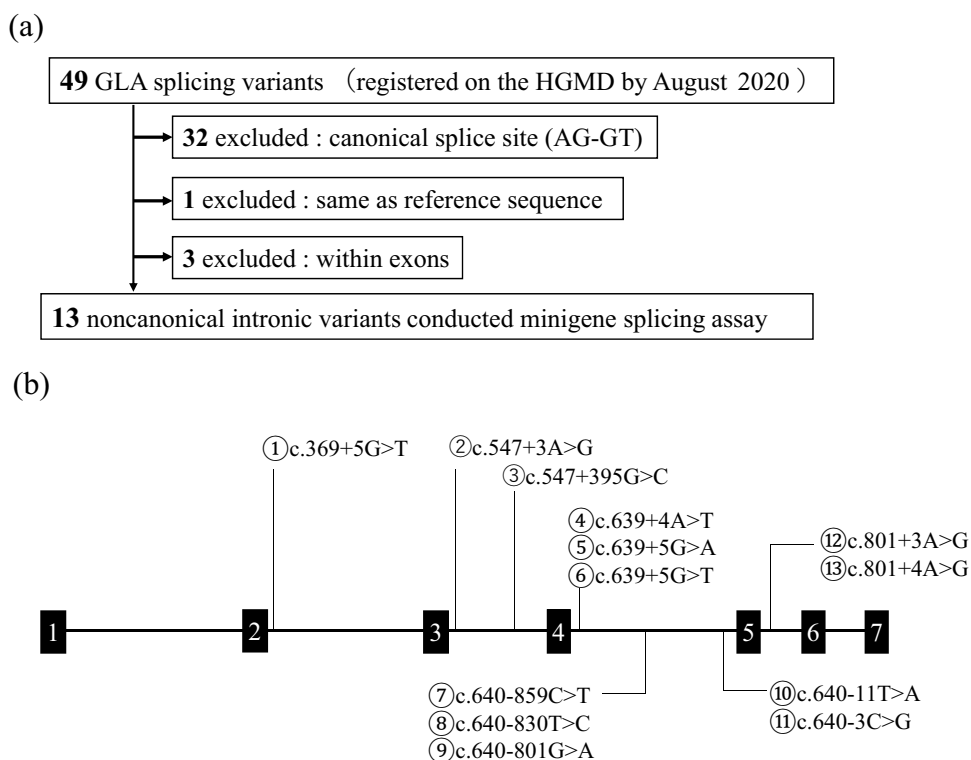
Recently, various bioinformatics tools have been developed to predict the possible pathogenic effects of missense and intronic variants [6, 7]; however, these predictions are not always correct. Presently, transcriptional analysis of patient samples is the most appropriate method for identifying splicing aberrations. However, RNA from affected organs is not always available. Moreover, it is often difficult to analyze mRNA obtained from peripheral leukocytes owing to low content and fragility. As an alternative, minigene splicing analyses have been developed [8–14]. In this study, we performed a functional minigene splicing assay on the reported *GLA* non-canonical intronic variants to examine possible splicing defects.

Materials and methods

Variant nomenclature and selection of non-canonical splice site variants

GLA variants were numbered according to the guidelines of the Human Genome Variation Society (<https://www.hgvs.org/mutnomen>) using the NCBI Reference Sequence NM_000169.3. Candidate variants for minigene analysis were selected from HGMD Professional. By August 2020, 49 variants had been identified as splicing substitutions that caused splicing abnormalities. Among these, 32 variants were located at canonical splice sites, while three exonic variants were excluded. In addition, one variant was excluded because of suspected erroneous registration of the its information in the HGMD database. Therefore, we analyzed the remaining 13 *GLA* intronic variants (Fig. 1a). Among these, nine variants were adjacent to exons that did not contain AG-GT canonical splice sites, and the other four were located more than 100 nucleotides away from the nearest exon–intron junction, typically referred to as deep introns (Fig. 1b). To prove that minigene analysis had accurately detected splicing aberrations, the intronic variant (c.640-16A>G), considered a single-nucleotide polymorphism (SNP), was analyzed as a negative control. The allele

Fig. 1 **a** Selection of the candidate variants. **b** Location of each variant in the *GLA* gene



frequency of the variant in different population databases is 13.9% (gnomAD), 16.1% (1000G), and 7.7% (HGVD).

Bioinformatics analysis

To predict potential alterations in the donor/acceptor splice sites, we used the following tools: SpliceSiteFinder-like (<https://www.interactive-biosoftware.com>), MaxEntScan (https://genes.mit.edu/burgelab/maxent/Xmaxentscan_score_seq.html), and NNSPLICE (https://www.fruitfly.org/seq_tools/splice.html) via Alamut software v.2.11 (Interactive Biosoftware, Rouen, France; <https://www.interactive-biosoftware.com>). The default settings were used for all predictions. Each tool was assumed to predict altered splicing when the change in splice site score was $\geq 10\%$ (MaxEntScan) or $\geq 5\%$ (SpliceSiteFinder-like and NNSPLICE) [15, 16]. The splicing process is regulated by splicing regulatory elements (SREs) that recruit various RNA-binding proteins [17]. SREs include intronic and exonic splicing enhancers (ISEs and ESEs) and silencers (ISSs and ESSs). Variants that alter the composition, affinity, or function of spliceosomes can lead to improper identification of exon–intron boundaries, thereby causing aberrant splicing [18]. To predict alterations in SREs, we used ESE-finder (<https://exon.cshl.edu/ESE/>) and RESCUE-ESE (<https://hollywood.mit.edu/burgelab/rescue-ese/>) within the Alamut software v.2.11 as well as HumanSplicingFinder (<https://umd.be/Redirect.html>).

Cell culture and minigene constructs

HEK293T and HeLa cells were cultured in DMEM and EMEM, respectively, with both media containing 10% fetal bovine serum and 1% penicillin–streptomycin (Fuji-film, Osaka, Japan). Wild-type genomic DNA fragments, including the targeted exon(s) and approximately 200 bp of surrounding introns, were amplified using Gflex DNA polymerase (Takara Bio, Shiga, Japan). Amplicons were subsequently cloned into the H492 vector based on the pcDNA3.0 mammalian expression vector (Invitrogen, Carlsbad, CA, USA) using the In-Fusion HD Cloning Kit (Takara Bio), according to the manufacturer’s instructions. Mutant plasmids were created via site-directed mutagenesis with the Prime STAR Mutagenesis Basal Kit (Takara Bio). The primer sequences used are listed in Supplementary Table S1. For deep intronic mutations (no. 7–9), cloning fragments were made via overlap extension polymerase chain reaction (PCR), followed by traditional restriction cloning using *NheI* and *BamHI* sites ligated with the DNA Ligation Kit Ver. 2.1 (Takara Bio), as described in Supplementary Fig. S1. Hybrid minigenes were transfected into HEK293T and HeLa cells using the Lipofectamine 3000 Transfection Kit (Thermo Fisher Scientific, Waltham, MA, USA). After 24 h, the total

RNA was extracted from the cells and purified using the RNeasy Plus Mini Kit (QIAGEN, Hilden, Germany). Total RNA was reverse-transcribed into cDNA using the EcoDry Premix (Double Primed; Takara Bio) and then subjected to PCR amplification using gene-specific primers YH307 and YH308 (Supplementary Table S1). The PCR products were analyzed using an Agilent 2100 Bioanalyzer system (Agilent Technologies, Santa Clara, CA, USA).

Data collection for transcriptome analysis of variant no. 9 (c. 640-801G>A)

Informed consent was obtained from the patient harboring mutation no. 9 (c.640-80G>A), whose blood sample was used for direct RNA sequencing. Total RNA was extracted using the RiboPure Blood Kit (Invitrogen) and an RNA stabilization agent (RNAlater; Invitrogen), after which a library was prepared using the SureSelect^{XT} RNA Direct Reagent Kit (Agilent Technologies). Briefly, mRNA obtained from the patient’s blood sample was randomly fragmented, and adaptor-ligated cDNA was synthesized using the SureSelect RNA Library Prep Kit, followed by PCR amplification to prepare cDNA library amplicons. The SureSelect RNA Target Enrichment Probe Library and cDNA library amplicons were hybridized using SureSelect^{XT} reagents and subjected to high-throughput sequencing using the MiSeq platform, as described in the Illumina manual (San Diego, CA, USA). The sequencing data were fed into the Strand NGS 4.0 software (Strand Life Sciences Pvt. Ltd., Bangalore, India) and visualized using the Integrative Genomics Viewer software (version 2.11.7) [19]. The cryptic exon inclusion ratio, or “percent spliced in” (PSI), describes the ratio of the cryptically spliced transcripts to the sum of both the cryptically and normally spliced transcripts. PSI was calculated according to the formula described by Sakaguchi et al. [20]. The PSI values ranged from 0 (completely skipped) to 1 (complete inclusion).

Results

Clinical phenotype

Although the clinical phenotype and enzymatic activity were not described for variant nos. 1 and 8, phenotypes were reported for the remaining 11 variants: nos. 2, 3, 4, 6, and 10–13 manifested as the classic type, whereas nos. 5, 7, and 8 were associated with later-onset or cardiac type. Variant no. 9 (c. 640-801G>A, often described as “IVS4+919G>A” or “c.639+919G>A”) was also identified in our genetic analysis cohort. The patient was an 81-year-old Japanese male who suffered from congestive heart failure. Neither detailed

clinical information nor residual enzymatic activity was available, and the patient did not undergo dialysis treatment.

Minigene splicing assay results

The minigene splicing assay revealed that all reported non-canonical intronic variants of *GLA* were associated with aberrant splicing (Table 1, Fig. 2, and Supplementary Fig. S2). We identified a partial deletion in the adjacent exon (nos. 1 and 2), exon skipping (os. 4–6, and 10), and partial inclusion of an adjacent intron (nos. 11–13). In addition, all deep intronic variants (os. 3–6) resulted in the creation of a cryptic exon. Regarding the protein effect, variant no. 10 exhibited a non-truncating defect (exon 10 consisted of 162 bp, a multiple of three), whereas the remaining variants caused truncating defects. Variant c.640-16A>G, considered to be an SNP, showed normal splicing (Supplementary Fig. S3).

Interpretation of variant pathogenicity and bioinformatics analysis for splicing defects

All variants were interpreted as having uncertain significance according to the ACMG guidelines [21] (Supplementary Table S2). Each in silico prediction tool for splice site score (SSF-like, MaxEntScan, and NNSPLICE) correctly predicted splicing defects for variants near splice sites (nos. 1, 2, 4–6, and 10–13). For deep intronic variants (nos. 3 and 7–9), splicing abnormalities could not be predicted by the tools that calculated changes in splice site score; however, except for variant no. 7, the in silico tools that predicted splicing defects based on alterations in SREs were effective for the deep intronic variants (Supplementary Table S3).

Direct RNA sequencing for variant no. 9 (c.640-801G>A)

The cryptic exon inclusion ratio (PSI) for the patient harboring variant no. 9 was 0.42, whereas that of the control was 0.027 (Supplementary Fig. S4).

Morality ratios of normal and aberrantly spliced transcripts for the deep intronic variants

For the deep intronic variants (nos. 3 and 7–9), the morality ratios of the normal and aberrantly spliced transcripts were determined using the 2100 Bioanalyzer Expert Software. The morality ratios differed between the HEK293T and HeLa cells in several variants as well as in the wild-type sample (Supplementary Table S4).

Discussion

In this study, we demonstrated that all reported non-canonical splice site variants in *GLA* were associated with aberrant splicing. As the pathogenicity of non-canonical splice variants is quite complex to interpret, all candidate variants in this study were classified as having uncertain significance according to the ACMG guidelines. Furthermore, in silico tools often cannot predict the possibility of aberrant splicing in intronic variants that do not involve canonical splice sites. Therefore, validating splicing effects with an *in vitro* splicing assay is useful for confirming pathogenicity and determining associations with clinical phenotypes.

Patients with nonsense canonical splice sites, or frameshift variants, exhibit protein-truncating defects and generally show a classic phenotype [22]. Variant nos. 1 and 2 generated transcripts that had partial deletions in adjacent exons, resulting in protein-truncating variants. Although the study reporting variant no. 1 did not describe a phenotype, it was known that the male patient harboring variant no. 2 showed a classical phenotype [23]. Variant nos. 4–6 are located near exon 4, and the minigene assay revealed that they all exhibited complete exon 4 (92 bp) skipping. Patients harboring variant nos. 4 and 6 had classic phenotypes [24, 25], whereas the patient with variant no. 5 exhibited a later-onset phenotype [26]; however, this report did not specify sex, and thus it cannot be determined whether this was a heterozygous female or hemizygous male patient.

The minigene assay for variant no. 10 revealed whole exon 5 (162 bp) skipping, resulting in an in-frame deletion; furthermore, patients with variant no. 10 reportedly showed a classic phenotype [27]. Riera et al. investigated *GLA* sequence conservation patterns and revealed that amino acid residues 253–271, located near the active site, were highly conserved regions among multiple species [28]. Notably, variant no. 10 caused the deletion of residues 214–267, which may explain the classic phenotype. Variant no. 11 generated a transcript with 2 bp of intron 4 included, resulting in a frameshift mutation, another reasonable explanation for the classic phenotype [29]. The minigene assay for variant nos. 12 and 13 led to partial inclusion (36 bp) of intron 5, which initially appeared to be an in-frame insertion but was later found to create a stop codon in the fourth amino acid downstream of exon 5. Therefore, patients with these variants reportedly exhibited the classic phenotype [30]. For variant no. 12, the minigene assay results differed from those of the RT-PCR using the patients' mRNA, possibly because of the hybrid minigene construction. Recent research indicates that splicing regulatory elements are typically within 200–300

Table 1 Phenotype and results of RT-PCR and minigene assay of the candidate variants

No	variant	Intron	References	Phenotype (hemizygous)	α -Gal A activity (normal range)	RT-PCR analysis	Minigene assay		
							Splicing outcome	RNA effect	Protein effect
1	c.369+5 G>T	2	[43]	ND	ND	ND	Partial deletion of exon 2 (116 bp)	r.254_369del	p.Tyr86Serfs*16
2	c.547+3 A>G	3	[23]	Classic	1.7 nmol/mg/h (17.6–57.6)	ND	Partial deletion of exon 3 (62 bp)	r.486_547+1del	p.Gly163Leufs*2
3	c.547+395G>C	3	[31]	Classic	5.06 nmol/mg/h (169.5–212.7)	Cryptic exon (115 bp)	<ul style="list-style-type: none"> • Cryptic exon (115 bp) • Normal transcripts 	r.547_548ins115	p.Tyr-184Glufs*39
4	c.639+4 A>T	4	[24]	Classic	1.0 U/mL (no data)	ND	Skipping of exon 4 (92 bp)	r.548_639del	p.Gly-183Alafs*18
5	c.639+5 G>A	4	[26]	(Later-onset*)	ND	ND	Skipping of exon 4 (92 bp)	r.548_639del	p.Gly-183Alafs*18
6	c.639+5 G>T	4	[25]	Classic	0.2 nmol/h/mL (>0.3)	ND	Skipping of exon 4 (92 bp)	r.548_639del	p.Gly-183Alafs*18
7	c.640–859 C>T	4	[32]	Classic	0.5 nmol/mg/h (25–75)	Cryptic exon (57 bp)	<ul style="list-style-type: none"> • Cryptic exon (57 bp) • Normal transcripts 	r.639_640ins57	p.Lys213_Pro214ins10*
8	c.640–830T>C	4	[44]	ND	ND	ND	<ul style="list-style-type: none"> • Cryptic exon (57 bp) • Normal transcripts 	r.639_640ins57	p.Lys213_Pro214ins10*
9	c.640–801 G>A	4	[33]	Cardiac*	8.7 U/mg (9.1% of normal)	Cryptic exon (57 bp)	<ul style="list-style-type: none"> • Cryptic exon (57 bp) • Normal transcripts 	r.639_640ins57	p.Lys213_Pro214ins10*
10	c.640–11T>A	4	[27]	Classic*	0.02% of normal	Skipping of exon 5 (162 bp)	skipping of exon 5 (162 bp)	r.640_801del	p.Pro214_Met-267del
11	c.640–3 C>G	4	[29]	Classic#	ND	ND	Partial inclusion of intron 4 (2 bp)	r.640-1_640ins2	p.Pro214Serfs*27
12	c.801+3 A>G	5	[30]	Classic*	0.5 (no unit description)	<ul style="list-style-type: none"> • Partial inclusion of intron 5 (66 bp) • Entire intron 5 (217 bp) 	Partial inclusion of intron 5 (36 bp)	r.801_802ins36	p.Met267_Leu268ins4*
13	c.801+4 A>G	5	[30]	Classic*	ND	ND	Partial inclusion of intron 5 (36 bp)	r.801_802ins36	p.Met267_Leu268ins4*

ND not described

*Sex unknown

#Female

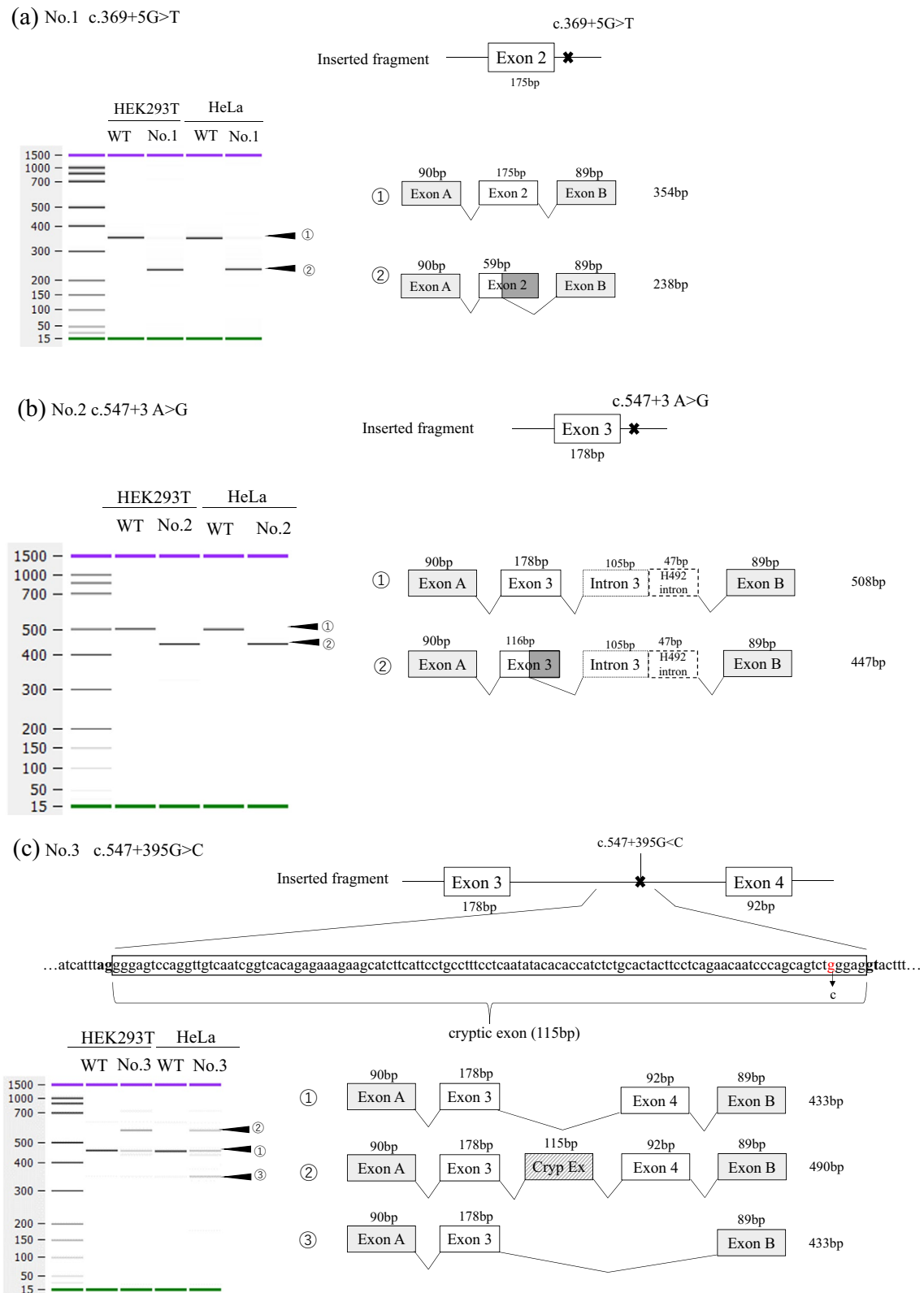


Fig. 2 Results of transcriptional analysis using the splicing minigene assay. The left part shows the electropherogram obtained with the bioanalyzer. The upper right part shows each inserted fragment constructed with individual exons and flanking introns. The lower right part shows a schematic representation of the splicing outcome **a** No. 1

c.369+5G>T. **b** No. 2 c.547+3A>G. **c** No. 3 c.547+395G>C. **d** No. 4 c.639+4A>T, no. 5 c.639+5G>A, and no. 6 c.639+5G>T. **e** No. 7 c.640–859 C>T, no. 8 c.640–830T>C, and no. 9 c.640–801 G>A. **f** No. 10 c.640–11T>A, no. 11 c.640–3 C>G, no. 12 c.801+3 A>G, and no. 13 c.801+4 A>G

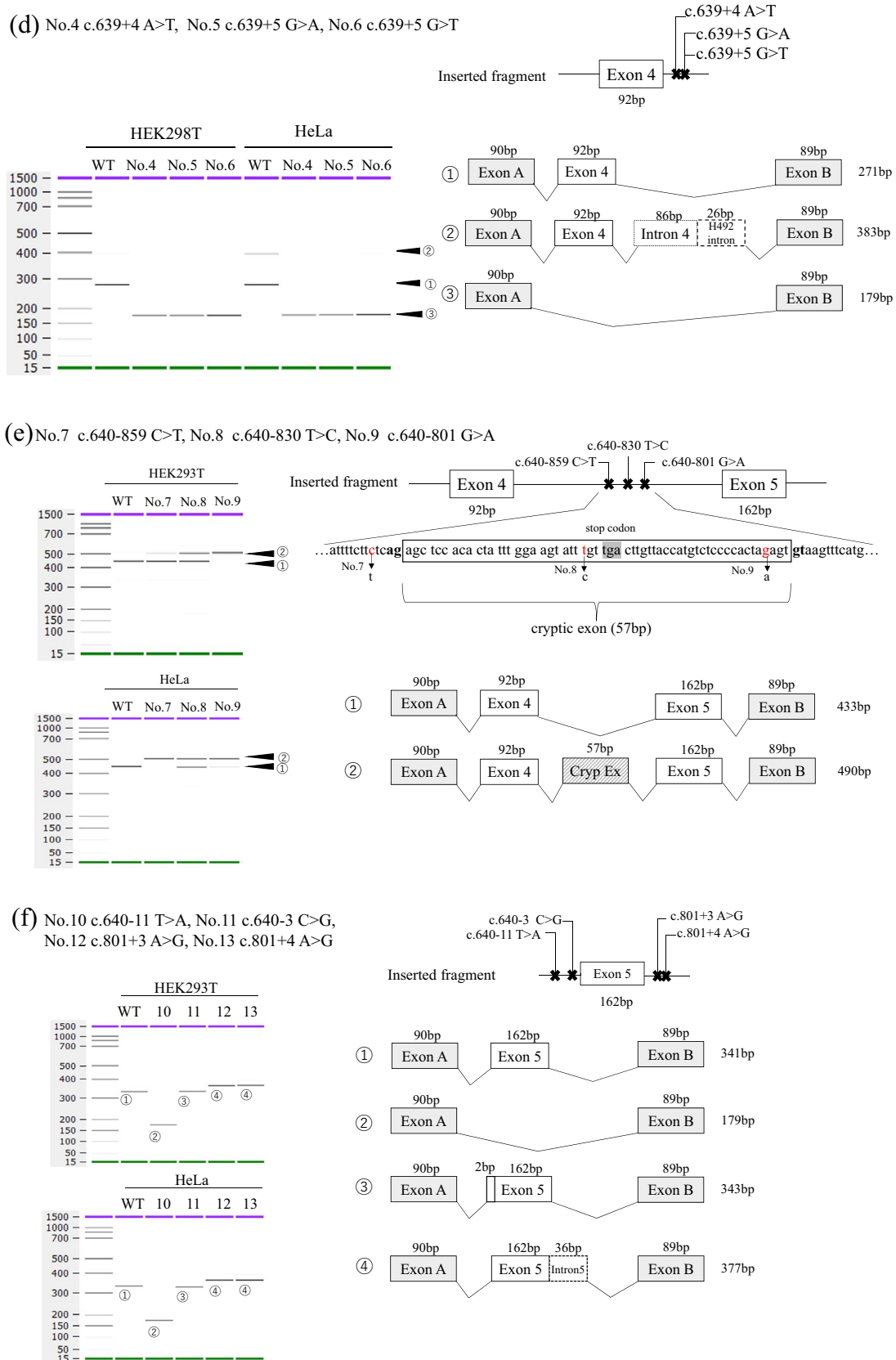


Fig. 2 (continued)

nucleotides upstream and/or downstream of the regulated exon [31]. Therefore, considering intron 5 is a short intron, 140 nucleotides downstream of exon 5 could have been included when making the fragment in this study.

Variant nos. 3 and 7–9 were deep intronic variants that created cryptic exons, which were in the vicinity of the variants. These variants caused protein-truncating defects; the cryptic exon resulting from variant no. 3 consisted of 115 bp nucleotides, leading to frameshift insertion, whereas those resulting from variant nos. 7–9 contained premature-termination codons. The clinical phenotype, however, differed between the variants. Patients with variant nos. 3 and 7 exhibited the classic type [32, 33], while variant no. 9 caused a milder cardiac phenotype [34]. The direct RNA sequence of variant no. 9 revealed that the cryptic exon inclusion ratio (PSI) was 0.42, suggesting that approximately 60% of the transcripts were still normally spliced. This generation of normal and abnormal transcripts may, thus, reduce disease severity [35]. In addition, the morality ratios of normal and aberrantly spliced transcripts for variant nos. 3 and 7–9 differed from those in HEK293T and HeLa cells. Moreover, different cell types have different α Gal A activity cutoffs [36]. Dai et al. [37] reported another deep intronic variant (c.639+1326C>T) detected in a male patient with Fabry disease who had the renal phenotype with a mild α Gal A deficiency (75% of normal control). The mRNA extracted from his peripheral blood lymphocytes was subjected to RT-PCR, which revealed normal transcripts and two types of abnormally spliced transcripts (both were truncating types). The aberrantly spliced transcripts encoded deficient α Gal A with about 25% of wild-type α Gal A activity. The high residual α Gal A activity was considered to be caused by normal transcript expression (a quarter of the total transcripts) and activity level of α Gal A encoded by the abnormally spliced transcripts.

Notably, variant no. 9, which causes the cardiac type, has a high prevalence, especially in Taiwan (1 in 2810 people) [38]. Interestingly, Chiang et al. reported that the rates of variant carriers did not differ among healthy controls, people with type 2 diabetes, and people with cardiac disease in Taiwan [39]. A minigene assay was conducted in seven types of human cell lines, which revealed that variant no. 9 influenced alternative splicing in a tissue-specific manner [39]. Recent studies also found modulation of alternative splicing using antisense RNAs [40] and amiloride [41]. Thus, it is important to correctly identify mutations that cause aberrant splicing and verify the underlying mechanisms. Moreover, minigene analysis of single-nucleotide substitutions in introns with high allele frequencies, which were considered SNPs, showed normal splicing. This further confirms that minigene analysis correctly determines splicing abnormalities.

This study had several limitations. First, except for variant no. 9, the validated variants were not from our cohort but rather from reported cases. These are often less descriptive regarding clinical data, such as the Mainz Severity Score Index, which is widely used to indicate the clinical severity of Fabry disease [42]. Second, *in vivo* validation using patient samples was insufficient other than that for no. 9. Finally, as the hybrid plasmids used for the minigene splicing assay were constructed artificially, the assay did not always imitate the *in vivo* splicing reaction. However, several previous studies performed transcriptional analyses via RT-PCR using patient mRNA, which mostly produced results consistent with ours [32–34].

In conclusion, our study revealed and confirmed splicing defects in 13 variants of the *GLA* gene. This analysis of splicing aberrations established correlations with pathogenicity and may contribute to elucidating tissue-specific splicing mechanisms.

Supplementary Information The online version contains supplementary material available at <https://doi.org/10.1007/s10157-023-02361-x>.

Acknowledgements The authors wish to thank all study participants, their social guardians, and primary doctors. We are profoundly grateful to Mrs. Yoshimi Nozu and Ming Juan Ye (Kobe University) for their technical assistance. We greatly appreciate Mr. Daichi Yamasoba (Kobe University) for technical advice on plasmid construction.

Funding Open access funding provided by Kobe University. This work was supported by the Kawano Masanori Memorial Public Interest Incorporated Foundation for Promotion of Pediatrics to T.H.

Data availability statement The data are not publicly available to maintain the confidentiality of patients' details but can be obtained from the corresponding author upon reasonable request.

Declarations

Conflict of interest The authors have declared that no conflict of interest exists.

Ethical approval All procedures performed in this study were carried out according to the ethical standards of the Institutional Review Board of Kobe University Graduate School of Medicine (IRB approval nos. 65 and 301) and with the 1964 Helsinki Declaration and its later amendments on comparable ethical standards. Comprehensive informed consent was obtained from all participants in the study and/or their guardians regarding the use of the patients' clinical data.

Open Access This article is licensed under a Creative Commons Attribution 4.0 International License, which permits use, sharing, adaptation, distribution and reproduction in any medium or format, as long as you give appropriate credit to the original author(s) and the source, provide a link to the Creative Commons licence, and indicate if changes were made. The images or other third party material in this article are included in the article's Creative Commons licence, unless indicated otherwise in a credit line to the material. If material is not included in the article's Creative Commons licence and your intended use is not permitted by statutory regulation or exceeds the permitted use, you will need to obtain permission directly from the copyright holder. To view a copy of this licence, visit <http://creativecommons.org/licenses/by/4.0/>.

References

- Brady RO, Gal AE, Bradley RM, Martensson E, Warshaw AL, Laster L. Enzymatic defect in Fabry's disease: ceramidetrihexosidase deficiency. *N Engl J Med*. 1967;276:1163–7.
- Germain DP. Fabry disease. *Orphanet J Rare Dis*. 2010;5:30.
- Nakao S, Takenaka T, Maeda M, Kodama C, Tanaka A, Tahara M, et al. An atypical variant of Fabry's disease in men with left ventricular hypertrophy. *N Engl J Med*. 1995;333:288–93.
- Elleder M, Bradová V, Smíd F, Buděšínský M, Harzer K, Kustermann-Kuhn B, et al. Cardiocyte storage and hypertrophy as a sole manifestation of Fabry's disease. Report on a case simulating hypertrophic non-obstructive cardiomyopathy. *Virchows Arch A Pathol Anat Histopathol*. 1990;417:449–55.
- Nakao S, Kodama C, Takenaka T, Tanaka A, Yasumoto Y, Yoshida A, et al. Fabry disease: detection of undiagnosed hemodialysis patients and identification of a “renal variant” phenotype. *Kidney Int*. 2003;64:801–7.
- Anna A, Monika G. Splicing mutations in human genetic disorders: examples, detection, and confirmation. *J Appl Genet*. 2018;59:253–68.
- Thusberg J, Olatubosun A, Vihinen M. Performance of mutation pathogenicity prediction methods on missense variants. *Hum Mutat*. 2011;32:358–68.
- Jian X, Boerwinkle E, Liu X. In silico tools for splicing defect prediction: a survey from the viewpoint of end users. *Genet Med*. 2014;16:497–503.
- Yamamura T, Horinouchi T, Aoto Y, Lennon R, Nozu K. The contribution of COL4A5 splicing variants to the pathogenesis of X-linked Alport syndrome. *Front Med (Lausanne)*. 2022;9:841391.
- Horinouchi T, Nozu K, Yamamura T, Minamikawa S, Omori T, Nakanishi K, et al. Detection of splicing abnormalities and genotype-phenotype correlation in X-linked Alport syndrome. *J Am Soc Nephrol*. 2018;29:2244–54.
- Tsuji Y, Yamamura T, Nagano C, Horinouchi T, Sakakibara N, Ishiko S, et al. Systematic review of genotype-phenotype correlations in Frasier syndrome. *Kidney Int Rep*. 2021;6:2585–93.
- Aoto Y, Horinouchi T, Yamamura T, Kondo A, Nagai S, Ishiko S, et al. Last nucleotide substitutions of COL4A5 exons cause aberrant splicing. *Kidney Int Rep*. 2022;7:108–16.
- Rossanti R, Horinouchi T, Yamamura T, Nagano C, Sakakibara N, Ishiko S, et al. Evaluation of suspected autosomal Alport syndrome synonymous variants. *Kidney360*. 2022;3:497–505.
- Inoue T, Nagano C, Matsuo M, Yamamura T, Sakakibara N, Horinouchi T, et al. Functional analysis of suspected splicing variants in CLCN5 gene in Dent disease 1. *Clin Exp Nephrol*. 2020;24:606–12.
- Tang R, Prosser DO, Love DR. Evaluation of bioinformatic programmes for the analysis of variants within splice site consensus regions. *Adv Bioinform*. 2016;2016:5614058.
- Wai HA, Lord J, Lyon M, Gunning A, Kelly H, Cibin P, et al. Blood RNA analysis can increase clinical diagnostic rate and resolve variants of uncertain significance. *Genet Med*. 2020;22:1005–14.
- Wang Z, Burge CB. Splicing regulation: from a parts list of regulatory elements to an integrated splicing code. *RNA*. 2008;14:802–13.
- Wang GS, Cooper TA. Splicing in disease: disruption of the splicing code and the decoding machinery. *Nat Rev Genet*. 2007;8:749–61.
- Robinson JT, Thorvaldsdóttir H, Winckler W, Guttman M, Lander ES, Getz G, Mesirov JP. Integrative genomics viewer. *Nat Biotechnol*. 2011;29:24–6.
- Sakaguchi N, Suyama M. In silico identification of pseudo-exon activation events in personal genome and transcriptome data. *RNA Biol*. 2021;18:382–90.
- Richards S, Aziz N, Bale S, Bick D, Das S, Gastier-Foster J, et al. Standards and guidelines for the interpretation of sequence variants: a joint consensus recommendation of the American College of Medical Genetics and Genomics and the Association for Molecular Pathology. *Genet Med*. 2015;17:405–24.
- Ortiz A, Germain DP, Desnick RJ, Politei J, Mauer M, Burlina A, et al. Fabry disease revisited: management and treatment recommendations for adult patients. *Mol Genet Metab*. 2018;123:416–27.
- Seo J, Kim M, Hong GR, Kim DS, Son JW, Cho IJ, et al. Fabry disease in patients with hypertrophic cardiomyopathy: a practical approach to diagnosis. *J Hum Genet*. 2016;61:775–80.
- Topaloglu AK, Ashley GA, Tong B, Shabbeer J, Astrin KH, Eng CM, et al. Twenty novel mutations in the alpha-galactosidase A gene causing Fabry disease. *Mol Med*. 1999;5:806–11.
- Zizzo C, Monte I, Pisani A, Fatuzzo P, Riccio E, Rodolico MS, et al. Molecular and clinical studies in five index cases with novel mutations in the GLA gene. *Gene*. 2016;578:100–4.
- Choi JH, Lee BH, Heo SH, Kim GH, Kim YM, Kim DS, et al. Clinical characteristics and mutation spectrum of GLA in Korean patients with Fabry disease by a nationwide survey: underdiagnosis of late-onset phenotype. *Medicine*. 2017;96:e7387.
- Lee BH, Heo SH, Kim GH, Park JY, Kim WS, Kang DH, et al. Mutations of the GLA gene in Korean patients with Fabry disease and frequency of the E66Q allele as a functional variant in Korean newborns. *J Hum Genet*. 2010;55:512–7.
- Riera C, Lois S, Domínguez C, Fernandez-Cadenas I, Montaner J, Rodríguez-Sureda V, de la Cruz X. Molecular damage in Fabry disease: characterization and prediction of alpha-galactosidase A pathological mutations. *Proteins*. 2015;83:91–104.
- Nowak A, Mechtler TP, Hornemann T, Gawinecka J, Theswet E, Hilz MJ, Kasper DC. Genotype, phenotype and disease severity reflected by serum LysoGb3 levels in patients with Fabry disease. *Mol Genet Metab*. 2018;123:148–53.
- Shabbeer J, Yasuda M, Benson SD, Desnick RJ. Fabry disease: identification of 50 novel alpha-galactosidase A mutations causing the classic phenotype and three-dimensional structural analysis of 29 missense mutations. *Hum Genom*. 2006;2:297–309.
- Cooper TA. Use of minigene systems to dissect alternative splicing elements. *Methods*. 2005;37:331–40.
- Higuchi T, Kobayashi M, Ogata J, Kaneshiro E, Shimada Y, Kobayashi H, et al. Identification of cryptic novel α -galactosidase A gene mutations: abnormal mRNA splicing and large deletions. *JIMD Rep*. 2016;30:63–72.
- Filoni C, Caciotti A, Carraresi L, Donati MA, Mignani R, Parini R, et al. Unbalanced GLA mRNAs ratio quantified by real-time PCR in Fabry patients' fibroblasts results in Fabry disease. *Eur J Hum Genet*. 2008;16:1311–7.
- Ishii S, Nakao S, Minamikawa-Tachino R, Desnick RJ, Fan JQ. Alternative splicing in the alpha-galactosidase A gene: increased exon inclusion results in the Fabry cardiac phenotype. *Am J Hum Genet*. 2002;70:994–1002.
- Horinouchi T, Yamamura T, Minamikawa S, Nagano C, Sakakibara N, Nakanishi K, et al. Pathogenic evaluation of synonymous COL4A5 variants in X-linked Alport syndrome using a minigene assay. *Mol Genet Genom Med*. 2020;8:e1342.
- Oliveira JP, Ferreira S. Multiple phenotypic domains of Fabry disease and their relevance for establishing genotype-phenotype correlations. *Appl Clin Genet*. 2019;12:35–50.
- Dai X, Zong X, Pan X, Lu W, Jiang GR, Lin F. Identification and functional characterization of the first deep intronic GLA mutation (IVS4+1326C>T) causing renal variant of Fabry disease. *Orphanet J Rare Dis*. 2022;17:237.

38. Liao HC, Hsu TR, Young L, Chiang CC, Huang CK, Liu HC, et al. Functional and biological studies of α -galactosidase A variants with uncertain significance from newborn screening in Taiwan. *Mol Genet Metab.* 2018;123:140–7.
39. Chiang HL, Wang NH-H, Song IW, Chang CP, Wen MS, Chien YH, et al. Genetic epidemiological study doesn't support GLA IVS4+919G>A variant is a significant mutation in Fabry disease. *Mol Genet Metab.* 2017;121:22–7.
40. Ferri L, Covello G, Caciotti A, Guerrini R, Denti MA, Morrone A. Double-target antisense U1snRNAs correct mis-splicing due to c.639+861C>T and c.639+919G>A GLA deep intronic mutations. *Mol Ther Nucleic Acids.* 2016;5:e380.
41. Chang WH, Niu DM, Lu CY, Lin SY, Liu TC, Chang JG. Modulation the alternative splicing of GLA (IVS4+919G>A) in Fabry disease. *PLoS ONE.* 2017;12:e0175929.
42. Whybra C, Kampmann C, Krummenauer F, Ries M, Mengel E, Miebach E, et al. The Mainz Severity Score Index: a new instrument for quantifying the Anderson–Fabry disease phenotype, and the response of patients to enzyme replacement therapy. *Clin Genet.* 2004;65:299–307.
43. Auray-Blais C, Blais CM, Ramaswami U, Boutin M, Germain DP, Dyack S, et al. Urinary biomarker investigation in children with Fabry disease using tandem mass spectrometry. *Clin Chim Acta.* 2015;438:195–204.
44. Lee SH, Li CF, Lin HY, Lin CH, Liu HC, Tsai SF, Niu DM. High-throughput detection of common sequence variations of Fabry disease in Taiwan using DNA mass spectrometry. *Mol Genet Metab.* 2014;111:507–12.

Publisher's Note Springer Nature remains neutral with regard to jurisdictional claims in published maps and institutional affiliations.